Strongly anisotropic nonequilibrium phase transition in Ising models with friction

Sebastian Angst, Alfred Hucht, and Dietrich E. Wolf
Fakultät für Physik und CeNIDE, Universität Duisburg-Essen, D-47048 Duisburg, Germany
(Received 9 January 2012; published 16 May 2012)

The nonequilibrium phase transition in driven two-dimensional Ising models with two different geometries is investigated using Monte Carlo methods as well as analytical calculations. The models show dissipation through fluctuation induced friction near the critical point. We first consider high driving velocities and demonstrate that both systems are in the same universality class and undergo a strongly anisotropic nonequilibrium phase transition, with anisotropy exponent $\theta = 3$. Within a field theoretical ansatz the simulation results are confirmed. The crossover from Ising to mean field behavior in dependency of system size and driving velocity is analyzed using crossover scaling. It turns out that for all finite velocities the phase transition becomes strongly anisotropic in the thermodynamic limit.

DOI: 10.1103/PhysRevE.85.051120 PACS number(s): 05.70.Ln, 68.35.Af, 05.50.+q, 05.70.Fh

I. INTRODUCTION

The interest in magnetic contributions to friction due to spin correlations has strongly increased in recent years. One interesting aspect is the energy dissipation due to the formation of spin waves in a two-dimensional Heisenberg model induced by a moving magnetic tip [1–3], which can be of Stokes or Coulomb type depending on the intrinsic relaxation time scales [4]. On the other hand, magnetic friction occurs also in bulk systems moving relative to each other. Kadau *et al.* [5] used a two-dimensional Ising model, cut into two halves parallel to one axis and moved along this cut with the velocity v, to explore surface friction. The motion drives the system out of equilibrium into a steady state, leading to a permanent energy flux from the surface to the heat bath. This model exhibits a nonequilibrium phase transition, which has been investigated in several different geometries [6] by means of analytical treatment as well as Monte Carlo (MC) simulations. The critical temperature T_c of the considered models depends on the velocity v and has been calculated exactly for various geometries in the limit $v \to \infty$. In this limit the class of models show mean-field-like critical behavior. Subsequent investigations have been done in a variety of context, in particular for driven Potts models [7] and for rotating Ising chains of finite length [8].

The nature of nonequilibrium phase transitions is still a field of large interest, and simple models helping to explore this field are seldom. A very famous example is the driven lattice gas (DLG) [9–11], exhibiting a strongly anisotropic phase transition. Despite many similarities between the driven lattice gas and the Ising model with friction, there is an important difference: The order parameter is conserved in the former, while it is nonconserved in the latter model. A further class of models characterized by nonequilibrium phase transitions are sheared systems [12–14], experimentally accessible within the framework of binary liquid mixtures.

Like the driven lattice gas, the systems investigated in the following exhibit a strongly anisotropic phase transition, which is investigated by means of Monte Carlo (MC) simulations as well as a field theoretical ansatz. In addition, the case of finite velocities v is analyzed by means of crossover scaling, where a broad range of velocities and system sizes are analyzed. We show that for all $v > 0$ the considered models end up in the mean field class with strongly anisotropic correlations as soon as the system size exceeds a velocity-dependent crossover length $L_\times(v)$.

While a crossover behavior from Ising to mean-field class occurs in various thermodynamic systems such as ionic fluid [15,16] and spin systems with long-range interactions [17], to our knowledge such a crossover including a change from isotropic to strongly anisotropic behavior has not been investigated in detail. The paper is organized as follows: After introducing the model and geometries, we determine the anisotropy exponent for $v = \infty$ using MC simulations as well as a field theoretical model. Then we turn to finite velocities and present the crossover scaling analysis. Finally we discuss our results.

II. MODELS

The systems considered in this work are denoted 2d and $1+1$d and are shown in Fig. 1 (for a classification see Ref. [6]). The 2d system is a two-dimensional two-layer Ising model with $L_\parallel \times L_\perp \times 2$ lattice sites, where the two layers are moved relative to each other along the parallel direction. Each lattice site carries one spin variable $\sigma_{i,j,k} = \pm 1$, and only nearest-neighbor interactions are taken into account. Periodic boundary conditions are applied in both planar directions (i.e., $\sigma_{i,j,k} = \sigma_{i+L_\parallel,j,k} = \sigma_{i,j+L_\perp,k}$). In order to simulate a finite velocity v using Monte Carlo simulations the upper subsystem is moved v times by one lattice constant during each random sequential Monte Carlo sweep (MCS). Since one MCS corresponds to the typical time $t_0 \approx 10^{-8}$ s a spin needs to relax into the direction of its local Weiss field, and as the lattice constant is of the order $a_0 \approx 10^{-10}$ m, the velocity v is given in natural units $a_0/t_0 \approx 1$ cm/s.

Instead of moving the two layers against each other, we reorder the couplings between the subsystems with time to simplify the implementation [6]. Introducing a time-dependent displacement

$$\Delta(t) = vt, \tag{1}$$

which is increased by one after each $2L_\parallel L_\perp/v$ random sequential spin flip attempts, the Hamiltonian can be expressed

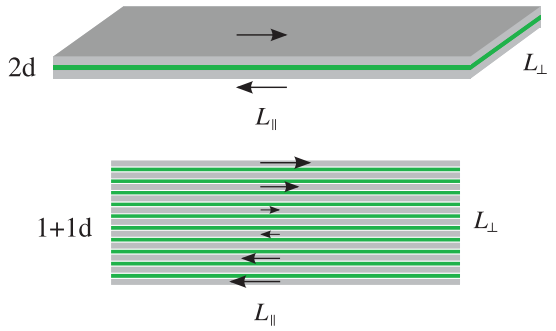

FIG. 1. (Color online) The systems considered in this work. The gray regions represent the magnetic systems, while the green (dark) regions are the moving boundaries. The arrows indicate the motion of the subsystems.

as

$$\beta\mathcal{H}(t) = -K\sum_{i=1}^{L_\parallel}\sum_{j=1}^{L_\perp}\sum_{k=0}^{1}\sigma_{i,j,k}(\sigma_{i+1,j,k}+\sigma_{i,j+1,k}) - K_\mathrm{b}\sum_{i=1}^{L_\parallel}\sum_{j=1}^{L_\perp}\sigma_{i,j,0}\sigma_{i+\Delta(t),j,1}, \quad (2)$$

with the reduced nearest neighbor coupling $K = \beta J$, the reduced boundary coupling $K_\mathrm{b} = \beta J_\mathrm{b}$, and $\beta = 1/k_\mathrm{B}T$. In the following we assume $J = J_\mathrm{b} = 1$.

The critical temperature $T_\mathrm{c}(v)$ of the regarded systems increases with v and saturates for high velocities. In the limit $v \to \infty$ an analytical calculation of the critical temperature for the 2d geometry yield

$$T_\mathrm{c}^{2\mathrm{d}}(\infty) = 4.058782423\ldots \quad (3)$$

for $J = J_\mathrm{b} = 1$ [6]. The basic idea of the analytic solution provides the approach for the implementation of infinite velocity, which works as follows: The interaction partner for a spin in the lower layer is chosen randomly from the same row in the upper layer. Thus we can use Eq. (2) with a random value $1 \leqslant \Delta(t) \leqslant L_\parallel$.

The $1+1$d system consists of a two-dimensional Ising model, where all rows are moved relative to each other. The displacement $\Delta(t) = vt$ as well as the coupling $K_\perp$ is equal for all adjacent rows, leading to the Hamiltonian

$$\beta\mathcal{H}(t) = -\sum_{i=1}^{L_\parallel}\sum_{j=1}^{L_\perp} K_\parallel\sigma_{i,j}\sigma_{i+1,j} + K_\perp\sigma_{i,j}\sigma_{i+\Delta(t),j+1}. \quad (4)$$

Again, periodic boundary conditions are applied in both directions, where discontinuities in $\perp$ direction are avoided through the homogeneous displacement $\Delta(t)$ [6]. The analytical treatment at $v \to \infty$ gave the critical temperature

$$T_\mathrm{c}^{1+1\mathrm{d}}(\infty) = 1/\ln\left(\tfrac{1}{2}\sqrt{3+\sqrt{17}}\right) = 3.46591\ldots \quad (5)$$

for $J_\parallel = J_\perp = 1$ in this case [6]. Within the scope of the $1+1$d model the velocity v corresponds to a shear rate, which is often denoted as $\dot{\gamma}$ [18,19]. However, we will use the term velocity for both driving mechanisms throughout this work.

In the following we argue that both systems show the same underlying critical behavior. In order to emphasize the similarity, Fig. 2 illustrates slight variations of both models. First of all we start with the $1+1$d model [Fig. 2(a)] and change every second bond perpendicular to the motion into a stationary bond. Additionally, we perform a transformation that changes the homogeneous shear $\Delta(t)$ into an alternating shift $\pm\Delta(t)$ of the double chains and reverses $(i \to -i)$ every second double chain, leading to the configuration in Fig. 2(b). These modifications do not change the critical behavior of the $1+1$d system, since still one-dimensional chains (now consisting of two rows) are moved relative to each other. On the other hand, the cross section of the 2d model can be visualized in a slightly different way [see Fig. 2(d)] without altering the corresponding Hamiltonian, Eq. (2). Since the next nearest double chains in Fig. 2(b) are not moving relative to each other, the only difference between Figs. 2(b) and 2(d) are the third nearest neighbor bonds in Fig. 2(d), which are irrelevant at the critical point where long-range correlations dominate. Hence we conclude that both systems belong to the same universality class.

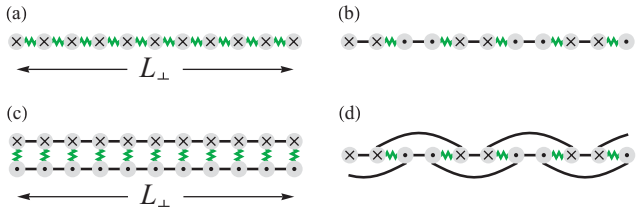

FIG. 2. (Color online) Cross sections of the $1+1$d (a) and the 2d model (c), and slight modifications of both models [(b) and (d)]. The gray circles represent spin chains and the connecting lines substitute for the coupling, where green wiggled lines stand for moving and black lines for stationary couplings. Black crosses and dots indicate a motion into and out of the plane, respectively.

Finally we mention that we must use the multiplicative rate

$$p_\mathrm{flip}(\Delta E) = e^{-\frac{\beta}{2}(\Delta E - \Delta E_\mathrm{min})}, \quad (6)$$

with $\Delta E_\mathrm{min} = \min(\{\Delta E\})$ to reproduce the critical temperatures, Eqs. (3) and (5), in simulations (for a discussion see Ref. [6]).

III. RESULTS

In order to illustrate symptomatic features of both systems, Fig. 3 shows a sequence of spin configurations of one layer of the 2d system (note that the same characteristics are observed in the $1+1$d system). On the left-hand side an equilibrated system at $T = 3.5$ well above the critical temperature of the nonmoving system, $T_\mathrm{c}^{2\mathrm{d}}(0) = 3.20755(5)$ [20], is presented. Shortly after starting the motion stripelike domains arise, spanning the whole system parallel to the motion. The stripes are rather stable, but are nonetheless transient, since they grow in time until the system ends up in a homogeneously magnetized state. The evolution in Fig. 3 is an example for a velocity-driven phase transition already described in Refs. [5,6], which is triggered by the onset of the motion and the associated increase of the critical temperature. The circumstances are comparable to a quench, which is characterized by a temperature decrease below T_c. After a quench a coarsening of domains is observed, whereas the growth of the domains can be described by a

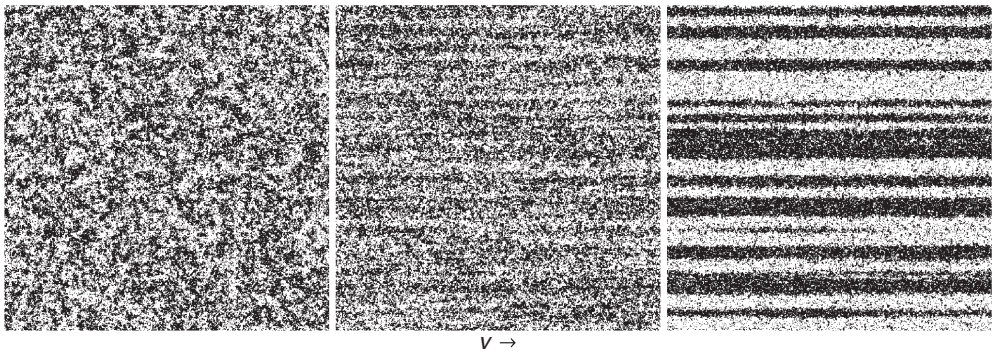

FIG. 3. Snapshots of one layer of the 2d model with $L_\parallel = L_\perp = 512$ and $J_\parallel = J_\perp = 1$ at temperature $T = 3.5$, which fulfills $T_c^{2d}(0) < T < T_c^{2d}(\infty)$. We start with an equilibrium system at $v = 0$ (left), set $v = \infty$, and show the evolution at $t = 42$ MCS (center) and $t = 360$ MCS (right).

power law (e.g., Refs. [21,22]). Domain growth in systems exhibiting a strongly anisotropic phase transition, e.g., the DLG model, is also a well-investigated subject [10,23,24]. The corresponding time evolution of spin configurations are similar to those shown in Fig. 3, leading to the assumption that the 2d and the $1+1$d geometries are also characterized by strongly anisotropic correlations, which is shown in the following section.

A. Determination of θ in the limit $v \to \infty$

A strongly anisotropic phase transition is characterized by a correlation length ξ_μ which diverges with direction dependent critical exponents ν_μ at the critical point [25],

$$\xi_\mu(t) \overset{t>0}{\sim} \hat{\xi}_\mu t^{-\nu_\mu}, \tag{7}$$

with direction $\mu = \{\perp, \parallel\}$ and reduced critical temperature $t = T/T_c - 1$. Defining the anisotropy exponent [26–28]

$$\theta = \frac{\nu_\parallel}{\nu_\perp}, \tag{8}$$

we find

$$\xi_\parallel(t)/\xi_\perp^\theta(t) \sim \hat{\xi}_\parallel/\hat{\xi}_\perp^\theta \tag{9}$$

independent of t. Isotropic scaling takes place for $\theta = 1$ and strongly anisotropic scaling is implied by $\theta \neq 1$. Several models with strongly anisotropic behavior where studied in the past. Examples are Lifshitz points as present in the anisotropic next nearest neighbor Ising (ANNNI) model [29,30], the nonequilibrium phase transition in the DLG [10], the two-dimensional dipolar in-plane Ising-model [28]. Furthermore, strongly anisotropic behavior usually occurs in dynamical systems, where the parallel direction can be identified with time and the perpendicular direction(s) with space [27,31]. In the latter case the anisotropy exponent θ corresponds to the dynamical exponent z.

The knowledge of the anisotropy exponent is essential and necessary for appropriate simulations of strongly anisotropic systems. To avoid complicated shape effects it is required to keep the generalized aspect ratio [26–28]

$$\rho = \frac{L_\parallel/\hat{\xi}_\parallel}{(L_\perp/\hat{\xi}_\perp)^\theta} \tag{10}$$

fixed, which requires the knowledge of θ. We will show in the following that the limit $\rho \to 0$ simplifies the analysis for infinite velocity v and turns out to be essential at finite v.

We first discuss the case $v \to \infty$ and always assume criticality, $t = 0$. In order to determine the anisotropy exponent θ we calculate the perpendicular correlation function $G_\perp(L_\parallel, L_\perp; r_\perp) = \langle \sigma_{i,j}\sigma_{i,j+r_\perp}\rangle$ between spins at distance $r_\perp$ in cylinder geometry $L_\perp \to \infty$ (leading to $\rho \to 0$), and thereby gain the correlation length $\xi_\perp(L_\parallel)$ through

$$G_\perp(L_\parallel, \infty; r_\perp) \sim \hat{G}_\perp(L_\parallel)\, e^{-r_\perp/\xi_\perp(L_\parallel)}, \tag{11}$$

where the prefactor $\hat{G}_\perp(L_\parallel)$ is shown to be proportional to $L_\parallel^{-2/3}$ in the Appendix. Approaching the critical point within the given geometry, the correlation length $\xi_\parallel(t)$ is limited by $L_\parallel$, and using Eq. (9) this leads to the relation

$$\xi_\perp(L_\parallel) \sim A_\perp L_\parallel^{1/\theta} \tag{12}$$

with nonuniversal amplitude $A_\perp$ [28,32]. Measuring the correlation length $\xi_\perp$ in dependency of the parallel extension $L_\parallel$ allows us to determine the anisotropy exponent θ.

In the simulations, the limit $L_\perp \to \infty$ is implemented by the condition $L_\perp/\xi_\perp \gtrsim 10$. This is sufficient to keep the systematic errors in $G_\perp$ smaller than the statistical error $\epsilon = 10^{-3}$ adequate to calculate $\xi_\perp$. From ϵ we can determine the required system sizes via $L_\perp/\xi_\perp = -2\ln[\epsilon/\hat{G}_\perp(L_\parallel)]$, where the factor 2 accounts for the periodic boundary conditions. As $\hat{G}_\perp \approx 0.1$ for $L_\parallel = 40$ and $\hat{G}_\perp \approx 0.02$ for $L_\parallel = 10^4$ for the $1+1$d model [see Fig. 4 (left)] we yield $L_\perp/\xi_\perp \approx 10$ for $L_\parallel = 40$ and $L_\perp/\xi_\perp \approx 0.7$ for $L_\parallel = 10^4$, meaning that for large systems a much smaller value of $L_\perp/\xi_\perp$ would be sufficient.

Figure 4 displays the correlation functions for both models. For the $1+1$d case these correlations are purely exponential also at short distances, since the coupling in $\perp$ direction is mediated through fluctuating fields [6], leading to dimensional reduction to an effectively one-dimensional system. The resulting correlation length $\xi_\perp$ is shown in the inset of Fig. 4 (left). The growth of $\xi_\perp(L_\parallel)$ follows a power law with exponent $\theta^{-1} = 1/3$ and with prefactor

$$A_\perp^{1+1d} = \lim_{L_\parallel \to \infty} L_\parallel^{-1/3}\xi_\perp^{1+1d}(L_\parallel) = 0.68(2), \tag{13}$$

indicated as a black line.

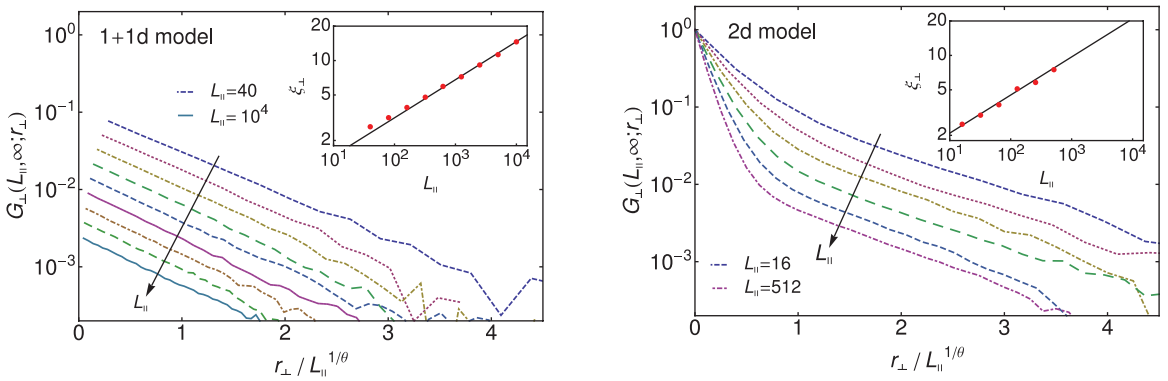

FIG. 4. (Color online) Rescaled correlation function $G_\perp(L_\parallel,\infty;r_\perp)$ at criticality for both models for varying system extensions, $L_\parallel = \{40,80,160,320,625,1250,2500,5000,10000\}$ (1 + 1d) and $L_\parallel = \{16,32,64,128,256,512\}$ (2d), respectively. The insets show $\xi_\perp(L_\parallel)$ whereby we yield $\xi_\perp$ by fitting an exponential function to the long-range part of $G_\perp(L_\parallel,\infty;r_\perp)$. The solid line is a power law with exponent $\theta^{-1} = 1/3$ as predicted by the field theoretical analysis (see text).

In the case of the 2d model (right figure in Fig. 4) we find two regions with different characteristics. The short-distance correlations are affected by the $\perp$ nearest-neighbor interactions within the planes, which are not present in the $1+1$d model. These correlations decay with a correlation length of the order $\xi_\perp^{\mathrm{eq}}[T_c^{2\mathrm{d}}(\infty)] \approx 1$. For large distances the correlations crossover to an exponential behavior. The exponential correlations are propagated by the fluctuations of stripelike domains. The analysis yields

$$A_\perp^{2\mathrm{d}} = \lim_{L_\parallel\to\infty} L_\parallel^{-1/3}\xi_\perp^{2\mathrm{d}}(L_\parallel) = 0.94(3) \tag{14}$$

in this case.

From the anisotropy exponent $\theta = 3$ we can derive the correlation length exponents $\nu_\parallel = 3/2$ and $\nu_\perp = 1/2$ using the generalized hyperscaling relation

$$2 - \alpha = 2\beta + \gamma = \nu_\parallel + (d-1)\nu_\perp, \tag{15}$$

with $d = 2$ and mean field exponents $\alpha = 0$, $\beta = 1/2$, and $\gamma = 1$, whose validity has been demonstrated in Ref. [6] by a mapping onto a mean field equilibrium model.

The calculation of θ in the limit $v \to \infty$ is done within a one-dimensional Ginzburg-Landau-Wilson (GLW) field theory [33]. For $v \to \infty$ it was shown in Ref. [6] that the $1+1$d model can be mapped onto an equilibrium system consisting of one-dimensional chains that only couple via fluctuating magnetic fields. Due to the stripe geometry with short length $L_\parallel$ and the periodic boundary conditions in $\parallel$ direction the magnetization is homogeneous in $\parallel$ direction, and parallel correlations are irrelevant. Hence we can use the zero mode approximation in this direction. However, it is necessary to include a term representing the interaction between adjacent spin chains. This can be expressed by the square of the spatial derivative of the magnetization in the direction $\perp$ to the motion. Hence the minimal GLW model to describe this strongly anisotropic mean field system is given by

$$\beta\mathcal{H} = L_\parallel \int_0^{L_\perp} dx \left(\frac{t}{2}m(x)^2 + \frac{1}{2}m'(x)^2 + \frac{u}{4!}m(x)^4\right) \tag{16}$$

with phenomenological parameters t and u, where $m(x)$ represents the magnetization of the spin chain at $\perp$ coordinate x. Equation (16) corresponds to the Hamiltonian used for the description of a cylinderlike spin system, which is infinite along one dimension, and finite and periodic in $d-1$ dimensions [33]. The partition function of Eq. (16) can be mapped onto a one-dimensional Schrödinger equation in a quartic anharmonic oscillator potential using a rescalation, which yields the critical exponents $\nu_\parallel = 3/2$ and $\theta = 3$. The detailed derivation is given in the Appendix.

B. Crossover scaling at finite velocities

We now turn to finite velocities. The following analysis is exemplarily done for the $1+1$d model, but as stated above, both models belong to the same universality class and similar results are expected for the 2d model. As we expect a crossover from an isotropic Ising model with $\theta = 1$ to a strongly anisotropic system with $\theta = 3$, we must be careful with the system geometry: We cannot use a fixed finite generalized aspect ratio ρ, Eq. (10), in the simulations, as θ is not constant. The only possible choice is $\rho \to 0$ (or $\rho \to \infty$), where the θ dependency drops out.

We consider the correlation length $\xi_\perp(t_c(v), v, L_\parallel)$ at reduced critical temperature

$$t_c(v) = \frac{T_c(v)}{T_c(0)} - 1, \tag{17}$$

where $T_c(0) = 2/\ln(\sqrt{2}+1)$. $t_c(v)$ is calculated via a finite-size scaling analysis of the perpendicular correlation length (not shown). As this procedure becomes inaccurate for small velocities $v < 2^{-8}$, we calculate the critical temperature according to

$$t_c(v) \overset{v\to 0}{\sim} \hat{c}\, v^\phi \tag{18}$$

with $\hat{c} = 0.29(1)$ in these cases, where we assume $\phi = 1/2$ in agreement with the literature [10,18,19]. The results are shown in the inset of Fig. 5(a).

Figure 5(a) shows the unscaled data, which gives evidence that the correlation length of systems moved at high velocities v are well described by the exponent $\theta = 3$ (dotted line), whereas for low velocities $v \lesssim 2^{-12}$ effectively the Ising exponent $\theta = 1$ (dashed line) holds for the simulated system sizes $L_\parallel$. The curvature of the data of intermediate velocities suggest the crossover. As a data collapse on the analytical known [34]

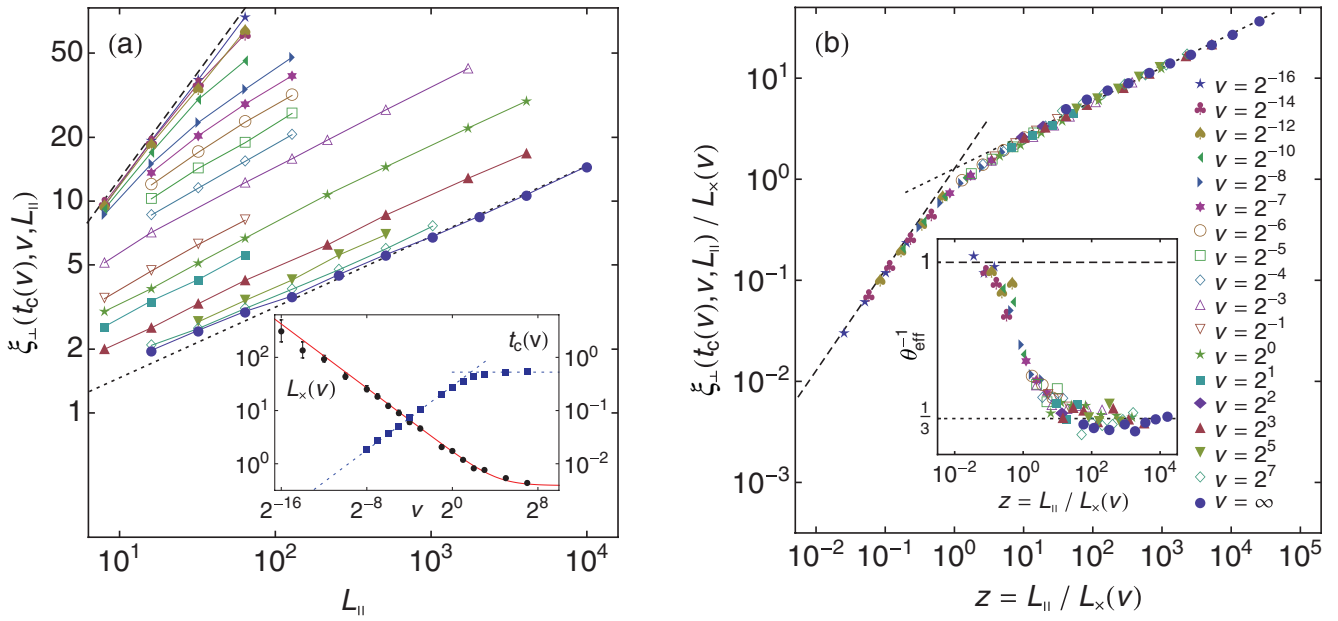

FIG. 5. (Color online) Velocity-dependent crossover behavior in the 1 + 1d case. Both pictures show log-log plots of the correlation length $\xi_\perp(t_c(v),v,L_\parallel)$ as function of the system size $L_\parallel$ at reduced critical temperature $t_c(v)$ for a broad range of different velocities v. The dashed line is the analytically known Ising limit $\xi_\perp(0,0,L_\parallel)/L_\parallel \sim 4/\pi$ valid for $v \to 0$ [34], while the dotted line has slope $\theta^{-1} = 1/3$. The left figure shows the unscaled data and the inset displays the rescaling factor $L_\times(v)$ for different velocities v (black dots, see text) and a function approximating the data given in Eq. (19), (red solid line) as well as the reduced critical temperature $t_c(v)$ (blue squares) together with its asymptotes, Eqs. (5) and (18). The right figure displays the same data rescaled with the crossover length $L_\times(v)$, leading to an excellent data collapse. The inset shows the crossover of the effective anisotropy exponent $\theta_{\rm eff}$ from $\theta_{\rm eff} = 1$ (Ising, dashed line) to $\theta_{\rm eff} = 3$ (MF, dotted line).

relation $\xi_\perp(0,0,L_\parallel)/L_\parallel \sim A^{\rm eq} = 4/\pi$ (dashed line in Fig. 5) has to be obtained in the limit $v \to 0$, both axes must be rescaled by the same factor $L_\times(v)$. This crossover length can be determined by applying the following method: We start with plotting the correlation length in the mean field limit $\xi_\perp[t_c(\infty),\infty,L_\parallel]$. Then we subsequently add the data for smaller v by rescaling $\xi_\perp$ and $L_\parallel$ with $L_\times^{-1}(v)$, which shifts the points parallel to the dashed line, until a data collapse is obtained [see Fig. 5(b)]. This procedure works quite accurate for velocities $v \gtrsim 2^{-3}$, only at very small $v \lesssim 2^{-12}$ the errors in $L_\times(v)$ grow due to the fact that we just shift the data along the dashed line. The resulting crossover length $L_\times(v)$ is pictured as black dots in the inset of Fig. 5(a). The behavior of $L_\times(v)$ is analogous to the velocity dependency of other quantities like the critical temperature or the energy dissipation, which are characterized by a power law for $v \ll 1$ and a saturation for $v \gg 1$.

We conclude that for all finite velocities $v > 0$ the critical behavior changes from Ising type to mean field type at a velocity dependent crossover length $L_\times(v)$ approximately given by

$$L_\times(v) \approx \left(\frac{A_\perp^{1+1{\rm d}}}{A^{\rm eq}}\right)^{3/2} \sqrt{1 + \frac{v_\times}{v}} \tag{19}$$

[solid red curve in the inset of Fig. 5(a)], where the velocity is measured in units 10^{-8} m/s and the size in 10^{-10} m. The velocity-independent prefactor was added to shift the crossover point (i.e., the intersection of the asymptotes) to $z = 1$. The saturation of $L_\times$ at $v_\times = 18(2)$ results from the lattice cutoff, as $L_\times(v_\times) \approx 1$. The inset in Fig. 5(b) shows the effective exponent $\theta_{\rm eff}$, obtained from the logarithmic derivative

$$\theta_{\rm eff}^{-1} = \frac{\partial \ln \xi_\perp}{\partial \ln L_\parallel}, \tag{20}$$

whose value changes from $\theta_{\rm eff} = 1$ (Ising, isotropic) to $\theta_{\rm eff} = 3$ (MF, strongly anisotropic). Note that we verified the mean field exponents for $v \gtrsim 1/8$ with finite-size scaling methods and also found good agreement of the scaling function with the universal finite-size scaling function [35] (not shown). In order to illustrate the change of the critical behavior, Fig. 6 shows typical critical spin configurations for different values of the crossover scaling variable $z = L_\parallel/L_\times(v)$.

We are now able to compare our results with the literature. If the crossover scaling variable $z \ll 1$ Ising-like behavior occurs, whereas for $z \gg 1$ mean field exponents and strongly anisotropic correlations are expected. In experiments [13], even slow shear rates of the order of 10^{-4} (in natural units t_0^{-1}, where now t_0 is the time scale of the fluid dynamics), lead to a crossover length $L_\times \lesssim 100$ and, as the typical system size is large with respect to the atomic distances, give $z \gg 1$, indicating that experimental data are always obtained in the mean field limit.

In relation to the results of Winter *et al.* [19] we find that the correlation length exponent has been measured in the regime $29 \lesssim z \lesssim 239$, leading to the anisotropy exponent $\theta \approx 3$ in agreement with our results. In Ref. [18] the correlation length exponents have also been determined in the mean field limit. Looking at the lowest velocity $v = 1/32$ we find $53 \lesssim z \lesssim 1066$, where a surprisingly small anisotropy exponent $\theta \approx 0.73$ has been estimated. The highest velocity $v = 50$ leads to $\theta \approx 1.2$ and $1100 \lesssim z \lesssim 22000$. These discrepancies might

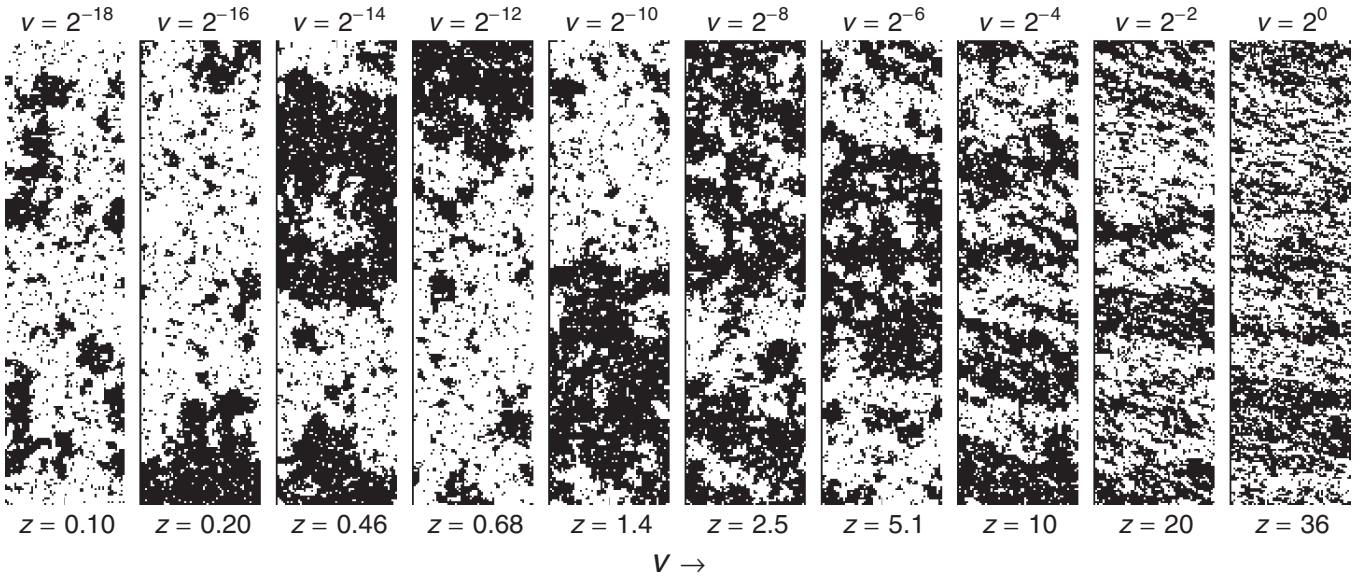

FIG. 6. Typical spin configurations of the critical $1+1$d system for $L_\parallel = 64$ and different velocities $v = 2^{-18}, \ldots, 1$. $z = L_\parallel / L_\times(v)$ denotes the crossover scaling variable (see text). The critical domains are isotropic and Ising-like for $z \ll 1$ and become anisotropic for $z \gtrsim 1$.

be attributed to the fact that an integral quantity, the order parameter, has been measured, as well as to strong surface effects induced by the open boundary conditions used in the $\perp$ direction.

IV. CONCLUSION

In this work we investigated two recently proposed driven Ising models with friction due to magnetic interactions, namely the $1+1$d and 2d model, using MC simulations as well as analytical methods. At first we focused on the strongly anisotropic critical behavior and calculated the anisotropy exponent θ in the limit of high driving velocity $v \to \infty$. Therefore the perpendicular correlation function of a cylinderlike geometry was calculated at criticality for different system sizes. Evaluating the connection between system size and correlation length, Eq. (12), we were able to find the critical exponents $\theta = 3$ as well as $\nu_\parallel = 3/2$ and $\nu_\perp = 1/2$. The analytic deviation of these exponents within the framework of a Ginzburg-Landau-Wilson Hamiltonian led to the same values. Comparing the results to the driven lattice gas [9,10] we note that it also shows a strongly anisotropic phase transition at a critical temperature, which grows with the velocity. Remarkably this phase transition is characterized by the same critical exponents at large fields.

Finally we focused on the critical behavior for finite velocities v and performed extensive MC simulations in order to calculate the crossover scaling function describing the crossover from the Ising universality class at $v = 0$ to the nonequilibrium critical behavior at $v \to \infty$. The analysis has exemplarily been done for the $1+1$d model, but as shown, both models belong to the same universality class and similar results are expected for the 2d model. In the analysis an additional complexity arose due to the strongly anisotropic characteristics of the correlations. Therefore we calculated the correlation length in a cylindrical system, circumventing intricate shape effects. We were able to identify a crossover length $L_\times(v)$ using a simple method based on the rescaling of data for each velocity such that a data collapse occurs. This procedure leads to an excellent data collapse of all simulation results for different velocities v and system sizes $L_\parallel$.

It turns out that for all finite velocities $v > 0$ the models undergo a crossover, at crossover length $L_\times(v)$, from an quasi-equilibrium isotropic Ising-like phase transition to a nonequilibrium mean-field behavior with strongly anisotropic correlations.

ACKNOWLEDGMENTS

We thank Felix M. Schmidt and Matthias Burgsmüller for valuable discussions. This work was supported by Coordenação de Aperfeiçoamento de Pessoal de Nível Superior - Deutscher Akademischer Austauschdienst (CAPES-DAAD) through the Project Related Exchange Brazil-Germany (PROBRAL) program as well as by the German Research Society (DFG) through SFB 616 "Energy Dissipation at Surfaces".

APPENDIX: SCALING EXPONENTS OF THE GINZBURG-LANDAU-WILSON MODEL

The following calculation is similar to Ref. [33]. Discretizing the integral

$$\beta\bar{\mathcal{H}} = L_\parallel \int_0^{L_\perp} dx \left(\frac{t}{2} m(x)^2 + \frac{1}{2} m'(x)^2 + \frac{u}{4!} m(x)^4 \right) \quad \text{(A1)}$$

with step size δx, $N \delta x = L_\perp$, $m_i = m(i\,\delta x)$, and $\delta m_i = m_{i+1} - m_i$ gives

$$\beta\bar{\mathcal{H}} = L_\parallel \sum_{i=1}^{N} \delta x \left(\frac{t}{2} m_i^2 + \frac{1}{2} \frac{\delta m_i^2}{\delta x^2} + \frac{u}{4!} m_i^4 \right). \quad \text{(A2)}$$

In order to evaluate the partition function

$$\mathcal{Z} = \int_{-\infty}^{\infty} \mathcal{D}[m(x)]\, e^{-\beta\bar{\mathcal{H}}}, \quad \text{(A3)}$$

we use abbreviations in analogy to transfer matrices,

$$T(m,m^+) = \underbrace{e^{-L_\parallel \delta x\left(\frac{t}{2}m^2+\frac{u}{4!}m^4\right)}}_{V(m)} \underbrace{\sqrt{\frac{L_\parallel}{2\pi\delta x}}e^{-\frac{L_\parallel \delta m^2}{2\delta x}}}_{U(\delta m)}, \quad \text{(A4)}$$

with $m^+ = m + \delta m$ to get

$$\mathcal{Z} = \int_{-\infty}^{\infty} dm_1 \int_{-\infty}^{\infty} dm_2 T(m_1,m_2) \int_{-\infty}^{\infty} dm_3 T(m_2,m_3) \times \cdots \times \int_{-\infty}^{\infty} dm_N T(m_{N-1},m_N) T(m_N,m_1) \quad \text{(A5)}$$

for the assumed periodic boundary conditions.

Let $x^+ = x + \delta x$ and $\psi(m^+)$ be the result of the integrations for the interval $]x^+, L_\perp]$. Since $T(m,m^+)$ is near-diagonal for $L_\parallel \to \infty$, we can write $\psi(m^+)$ as

$$\lambda\psi(m^+) \approx \psi(m) + \psi'(m)\delta m + \tfrac{1}{2}\psi''(m)\delta m^2, \quad \text{(A6)}$$

where λ denotes the growth factor of the integrations corresponding to the leading eigenvalue of the transfer matrix $T(m,m^+)$. The integral over m^+ in the partition function becomes

$$\begin{aligned}\psi(m) &= \int_{-\infty}^{\infty} dm^+ V(m) U(m^+ - m)\psi(m^+) \\ &= V(m)\sqrt{\frac{L_\parallel}{2\pi\delta x}} \int_{-\infty}^{\infty} dm^+ e^{-\frac{L_\parallel \delta m^2}{2\delta x}} \psi(m^+) \\ &= \frac{V(m)}{\lambda}\left(\psi(m) + \frac{\delta x}{2L_\parallel}\psi''(m)\right), \end{aligned} \quad \text{(A7)}$$

and yields the solution of the integrations for the interval $[x^+, L_\perp]$. Hence we get a differential equation for $\psi(m)$,

$$V(m)\left(\psi(m) + \frac{\delta x}{2L_\parallel}\psi''(m)\right) = \lambda\psi(m). \quad \text{(A8)}$$

We now substitute

$$\begin{aligned} \psi(m) &\to \Psi(\tilde{m}) && \text{(A9a)} \\ m &\to \tilde{m}\, u^{-1/6} L_\parallel^{-1/3} && \text{(A9b)} \\ \lambda &\to 1 - \Lambda\, \delta x\, u^{1/3} L_\parallel^{-1/3} && \text{(A9c)} \\ t &\to x\, u^{2/3} L_\parallel^{-2/3} && \text{(A9d)} \end{aligned}$$

and expand to lowest order around $L_\parallel = \infty$ to yield the Schrödinger equation in a quartic potential,

$$\left(-\frac{1}{2}\partial_{\tilde{m}}^2 + \frac{x}{2}\tilde{m}^2 + \frac{1}{4!}\tilde{m}^4 - \Lambda\right)\Psi(\tilde{m}) = 0, \quad \text{(A10)}$$

valid in the scaling limit $L_\parallel \to \infty$, $t \to 0$ with $x = t(L_\parallel/u)^{1/\nu_\parallel}$ kept fixed.

The correlation length $\xi_\perp(L_\parallel)$ is determined from the lowest eigenvalues $\Lambda_{0,1}$ of this equation, as

$$\xi_\perp = \delta x \left(\ln\frac{\lambda_0}{\lambda_1}\right)^{-1} \sim \frac{1}{\Lambda_1 - \Lambda_0}\left(\frac{L_\parallel}{u}\right)^{1/3}. \quad \text{(A11)}$$

From the substitution, Eqs. (A9), we directly read off the exponents $\nu_\parallel = 3/2$, and $\theta = 3$.

The correlation function amplitude $\hat{G}_\perp(L_\parallel)$ from Eq. (11) is proportional to m^2 and thus scales as $L_\parallel^{-2/3}$ as can be seen from Eq. (A9b).

[1] C. Fusco, D. E. Wolf, and U. Nowak, Phys. Rev. B **77**, 174426 (2008).
[2] M. P. Magiera, L. Brendel, D. E. Wolf, and U. Nowak, Europhys. Lett. **87**, 26002 (2009).
[3] M. P. Magiera, D. E. Wolf, L. Brendel, and U. Nowak, IEEE Trans. Magn. **45**, 3938 (2009).
[4] M. P. Magiera, S. Angst, A. Hucht, and D. E. Wolf, Phys. Rev. B **84**, 212301 (2011).
[5] D. Kadau, A. Hucht, and D. E. Wolf, Phys. Rev. Lett. **101**, 137205 (2008).
[6] A. Hucht, Phys. Rev. E **80**, 061138 (2009).
[7] F. Igloi, M. Pleimling, and L. Turban, Phys. Rev. E **83**, 041110 (2011).
[8] H. J. Hilhorst, J. Stat. Mech. Theor. Exp. (2011) P04009.
[9] S. Katz, J. L. Lebowitz, and H. Spohn, Phys. Rev. B **28**, 1655 (1983).
[10] B. Schmittmann and R. K. P. Zia, in *Phase Transitions and Critical Phenomena*, Vol. 17, edited by C. Domb and J. L. Lebowitz (Academic Press, London, 1995).
[11] R. K. P. Zia, J. Stat. Phys. **138**, 20 (2010).
[12] C. K. Chan and L. Lin, Europhys. Lett. **11**, 13 (1990).
[13] A. Onuki, J. Phys.: Condens. Matter **9**, 6119 (1997).
[14] E. N. M. Cirillo, G. Gonnella, and G. P. Saracco, Phys. Rev. E **72**, 026139 (2005).
[15] M. E. Fisher, J. Stat. Phys. **75**, 1 (1994).
[16] K. Gutkowski, M. A. Anisimov, and J. V. Sengers, J. Chem. Phys. **114**, 3133 (2001).
[17] E. Luijten, H. W. J. Blöte, and K. Binder, Phys. Rev. E **56**, 6540 (1997).
[18] G. P. Saracco and G. Gonnella, Phys. Rev. E **80**, 051126 (2009).
[19] D. Winter, P. Virnau, J. Horbach, and K. Binder, Europhys. Lett. **91**, 60002 (2010).
[20] A. Lipowski and M. Suzuki, Physica A **198**, 227 (1993).
[21] A. J. Bray, Adv. Phys. **43**, 357 (1994).
[22] R. Paul, S. Puri, and H. Rieger, Europhys. Lett. **68**, 881 (2004).
[23] C. Yeung, T. Rogers, A. Hernandez-Machado, and D. Jasnow, J. Stat. Phys. **66**, 1071 (1992).
[24] P. I. Hurtado, J. Marro, and E. V. Albano, Europhys. Lett. **59**, 14 (2002).
[25] Throughout this work, the symbol $\sim$ means asymptotically equal in the respective limit [e. g., $f(L) \sim g(L) \Leftrightarrow \lim_{L\to\infty} f(L)/g(L) = 1$]. Note that the variable t is used for the reduced temperature throughout the rest of this work.

[26] K. Binder, in *Finite Size Scaling and Numerical Simulations of Statistical Systems*, edited by V. Privman (World Scientific, Singapore, 1990), ch. 4.
[27] M. Henkel, *Conformal Invariance and Critical Phenomena* (Springer-Verlag, Berlin, 1999).
[28] A. Hucht, J. Phys A: Math. Gen. **35**, L481 (2002).
[29] W. Selke, Phys. Rep. **170**, 213 (1988).
[30] M. Pleimling and M. Henkel, Phys. Rev. Lett. **87**, 125702 (2001).
[31] H. Hinrichsen, Adv. Phys. **49**, 815 (2000).
[32] M. Henkel and U. Schollwock, J. Phys A: Math. Gen. **34**, 3333 (2001).
[33] E. Brézin and J. Zinn-Justin, Nucl. Phys. B, **257**, 867 (1985).
[34] J. L. Cardy, J. Phys A: Math. Gen. **17**, L385 (1984).
[35] D. Grüneberg and A. Hucht, Phys. Rev. E **69**, 036104 (2004).